

Chemical Modification of Wheat-Protein-Based Natural Polymers: Formation of Polymer Networks with Alkoxysilanes To Modify Molecular Motions and Enhance the Material Performance

Xiaoqing Zhang,* My Dieu Do, and Alex Bilyk

CSIRO Manufacturing and Materials Technology, Private Bag 33, Clayton South MDC, Clayton South, Victoria 3169, Australia

Received March 12, 2007; Revised Manuscript Received April 5, 2007

The mechanical performance of plasticized wheat gluten (WG) materials was significantly modified through the formation of different chemical and network structures with alkoxysilanes. The epoxy-functionalized alkoxysilanes were grafted to segments of WG, and then the condensation reactions between alkoxysilane segments occurred during thermal processing to form WG–siloxane networks. The mechanical properties and molecular motions of the networks were dependent on the amount and type of alkoxysilanes applied. A lower amount of alkoxysilanes caused the alkoxysilane molecules to predominately graft onto WG chains without forming linkages between WG segments, which produced an additional plasticizing effect on the WG systems with a longer elongation value and weaker tensile strength at relative humidity (RH) = 50% as compared to the WG system. However, such grafting improved the hydrostability of the materials and generated an improvement in tensile strength at RH = 85%. Increasing the amount of alkoxysilanes in the systems led to the formation of cross-linked WG–siloxane networks via linkages between alkoxysilane segments. Remarkable strength improvement was obtained for the networks with elongation values still higher than the original plasticized WG due to the flexible nature of the siloxane components. A more significant strength improvement was obtained for the WG–SiA systems at both RH = 50% and 85%, where SiA could form three-dimensional networks from siloxane condensation and generate highly cross-linked network structures with relatively low mobility. For WG–SiB systems, SiB could only form linear linkages, and the higher mobility of the SiB phase caused the systems to display a lower strength improvement with a longer elongation value.

1. Introduction

The search for material-specific applications for natural polymers is currently a topic of great interest because of the waning stocks of petrochemicals and therefore petrochemical polymers. The other advantage of these polymers is that they are easily absorbed into the environment by biological and natural physical degradation processes.^{1–3} Of particular interest in a series of our recent papers^{4–10} is a plant-protein-based natural polymer material, namely, wheat gluten (WG), which has applications in packaging, coatings/adhesives, or potentially as engineering plastics due to the toughness of the materials. A downside to the use of plant-based protein material is that their inherent properties are inferior to petrochemical-based systems. For this reason, chemical modification of raw agriculture products is necessary to improve the material properties and the processing capability.^{11–15} The methodology also plays a key role in enhancement of the hydrophobicity or hydrostability of the hydrophilic materials to provide high humidity (or water) resistance, thus extending their application.

One of the most effective ways to achieve mechanical strength improvement for protein-based films is chemical cross-linking. Aldehyde functional cross-linkers (formaldehyde, glyoxal, and glutaraldehyde) have been widely used in many protein-based materials, such as wheat gluten,^{16,17} soy proteins,^{18–20} collagen,²¹

corn zein,²² whey proteins,²³ cotton seed proteins,^{24,25} and even wool fibers,^{26,27} to promote the cross-linked network formed within the protein aggregated structures and to enhance the mechanical properties. Other cross-linkers such as carbodiimides,^{28,29} epoxy compounds,^{30,31} and genipin³¹ have also been studied for different protein systems, but it is the aldehyde-based cross-linkers that have provided the best performance improvements for proteins. However, the cross-linked protein systems investigated thus far usually do not display sufficient humidity resistance or barrier properties for water vapor.^{16,17} For example, in a recent study on thermal cross-linking WG with glyoxal,⁹ the mechanical properties of the resulting materials improved significantly (ca. 140% tensile strength improvement) under standard humidity conditions (relative humidity (RH) of 50%). The strength enhancement was minimal after exposure to high humidity conditions (RH = 85%) due to the hydrophilic nature of the chemical bonds formed in such cross-linking reactions.

As part of our continued effort in improving the properties of wheat-protein-based natural polymer materials,^{4–10} alkoxysilanes were applied to react with plasticized WG to form cross-linked networks in this work. Silanes have been used as organic or inorganic reactive agents to enhance the surface adhesion and “coupling” between organic and inorganic surfaces in composites.³² They have also been grafted onto polymers as cross-linking agents to improve the physical and mechanical properties of coatings and polymers^{33,34} and used in food packaging within the limits of good manufacturing practice

* Author to whom correspondence should be addressed. Phone: +61-3-95452653. Fax: +61-3-95441128. E-mail: Xiaoqing.Zhang@csiro.au.

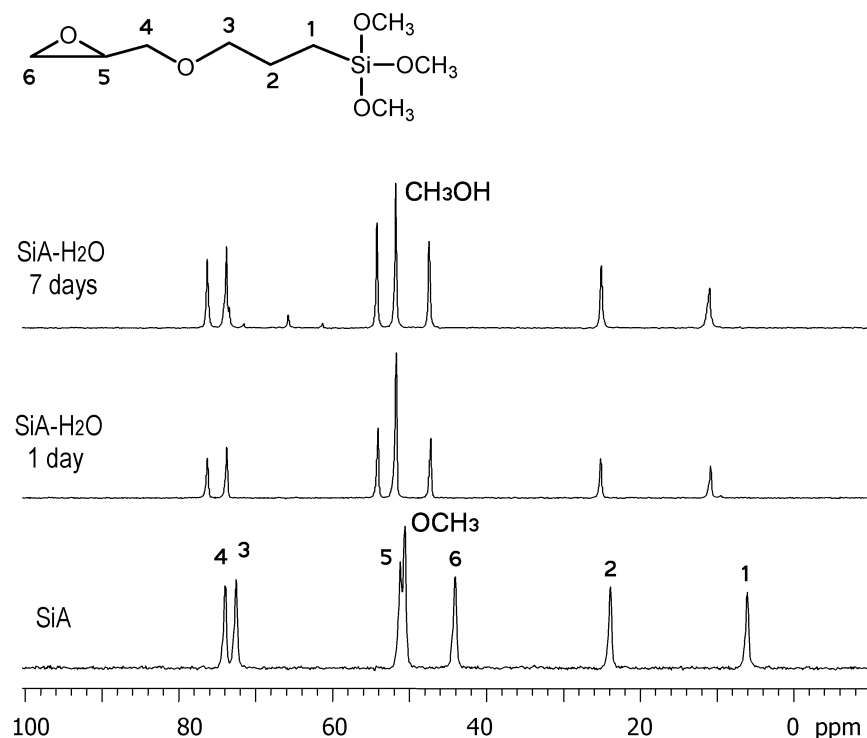
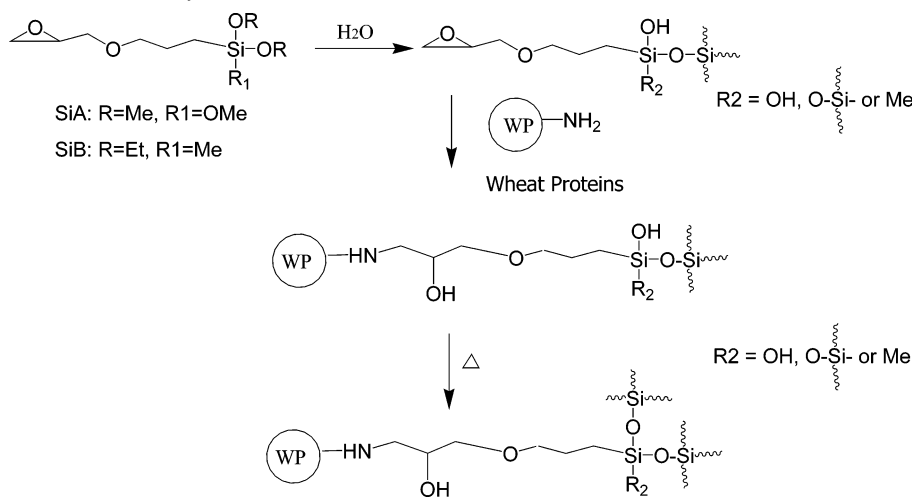


Figure 1. ^{13}C solution NMR spectra of pure SiA and SiA after hydration for 1 day or 7 days.

Scheme 1. Chemical Structures of Alkoxysilanes SiA and SiB and Their Reactions with Wheat Proteins



under Food and Drug Administration (FDA)-approved conditions.³⁵ The chemical structures of the two alkoxysilane compounds used in this study are shown in Scheme 1 and Figures 1 and 2. The bifunctional nature of SiA and SiB provides the possibility to form chemical linkages with various amino groups of wheat proteins via reactions with the glycidoxy groups. In addition, the tri- or dialkoxysilyl can be hydrolyzed by the water present as a plasticizer and then undergo polymerization via a condensation mechanism with other silane functional groups to form a silica-like network (as described in Scheme 1). The silica-like network can form on the surface of wheat proteins, thus potentially linking them with other protein particles in WG, or they can interpenetrate within a protein phase. Whichever the case, such an approach would improve the mechanical and hydrostability properties of the WG material. SiA is a silane with a trialkoxysilyl structure that has the potential of forming a three-dimensional intercon-

nected silane network, while SiB, a dialkoxy silane, can only form linear polymer segments in condensation reactions (Scheme 1).

It is expected that the changes in structure and motional states of the different phases in the WG–SiA and WG–SiB network will produce materials with different properties. High-resolution NMR spectroscopy was used to study the chemical reactions and structures formed between WG and alkoxysilanes. The mechanical performance of these WG–alkoxysilane materials under standard humidity ($\text{RH} \approx 50\%$) and high humidity ($\text{RH} \approx 85\%$) were examined. Dynamic mechanical analysis (DMA) was conducted to study the effect of formation of the WG–alkoxysilane network on mechanical performance, molecular motions, and transitions of the materials. This study provides an initial insight into the relationship between the structures of the network formed when WG is thermally reacted with SiA and SiB and the molecular motions and mechanical properties of the modified WG materials.

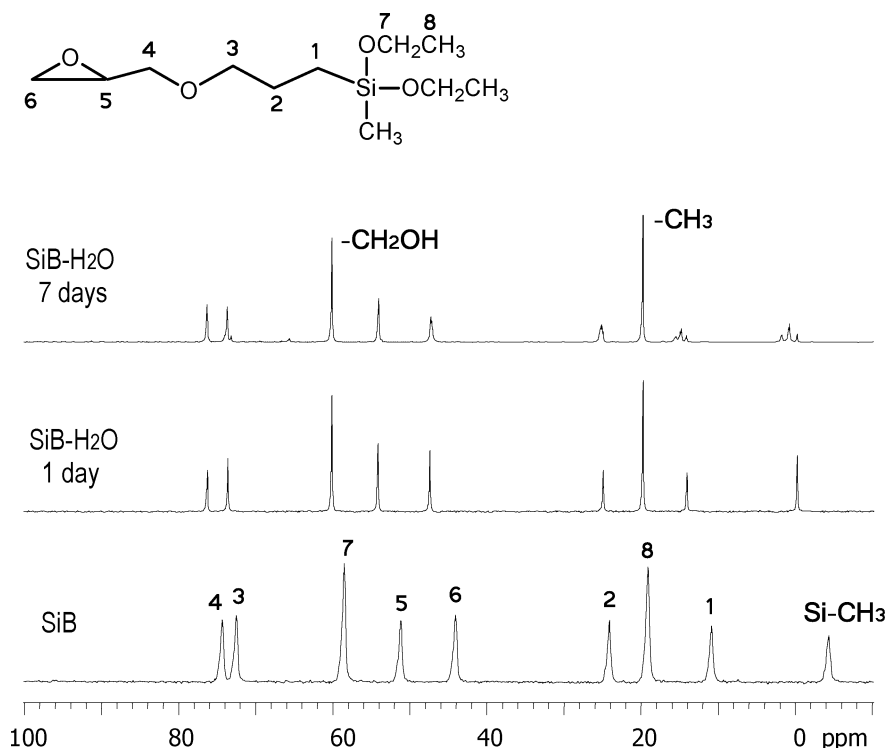


Figure 2. ^{13}C solution NMR spectra of pure SiB and SiB after hydration for 1 day or 7 days.

2. Experimental Section

2.1. Materials. Wheat gluten vital, supplied by Manildra Group Australia, contained about 80% proteins, 15% residual starch, 4% lipid, and around 1% fibers and other impurities on a dry basis. The moisture content was around 12%. Two alkoxy silane compounds glycidoxypyrpyl trimethoxy silane (SiA)³¹ and glycidoxypyrpyl methyldiethoxy silane (SiB) (Scheme 1) obtained from Dow Corning Co. and Sigma Aldrich, respectively, were used without further purification. Sheet samples of the WG system were prepared using water (14%) and glycerol (16%) as plasticizers. A small amount of Na_2SO_3 (0.3 wt % to WG) was added into all systems to dissociate the disulfide bonding within the protein chains to achieve efficient mixing between proteins and plasticizers. Either SiA or SiB was added into the plasticizer phase and homogeneously mixed with the plasticizers at varying amounts over a range from 1 to 8 wt % of silane with respect to the total mass of WG and plasticizer. Each sample formulation was mixed with a high-speed mixer operated at a speed of 3000 rpm for 1 min, left overnight, and then compression molded at an optimum temperature of 130 °C for 5 min using a heating press with a pressure of 12 tons. The sample size was 145 mm \times 145 mm with a thickness of 1.0 ± 0.1 mm. All samples were conditioned under either a standard humidity condition (RH = 50%) or a high humidity condition RH = 85% for 1 week, and then the weight loss, mainly the moisture content of each sample, was measured by drying the sample at 105 °C for 24 h ($\sim 12\%$ at RH = 50% and $\sim 22\%$ at RH = 85%).

2.2. Instrumentation. DMA experiments were operated on a Perkin-Elmer PYRIS Diamond DMA in dual cantilever bending mode at a frequency of 1 Hz. The temperature range was set at -100 to 150 °C with a heating rate of 2 °C/min. The storage modulus (E'), the loss modulus (E''), and $\tan \delta$ (E''/E') were recorded as a function of temperature throughout the experiment.

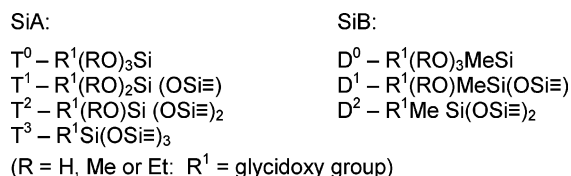
Mechanical properties of the samples were measured at room temperature and RH = 50% on an INSTRON 5566P with a cross-head speed of 50 mm/min, after conditioning the samples under either RH = 50% or RH = 85% at room temperature for 1 week. The samples after conditioning were sealed in polyethylene bags when moving from the conditioning tank to testing room, and the testing was conducted immediately. The data for each sample were obtained from an average

of testing 7–10 dog-bone-cut specimens with an effective length of 30 mm and width of 6 mm.

Solution ^{13}C and ^{29}Si NMR spectra were observed using a Varian Unity plus spectrometer at resonance frequencies of 75 MHz for ^{13}C , 60 MHz for ^{29}Si , and 300 MHz for ^1H . A 10 mm solution probe head was used, and nuclear Overhauser effect enhancement was applied to enhance the ^{13}C or ^{29}Si intensity. High-resolution solid-state NMR experiments were conducted at room temperature using the same spectrometer. ^{13}C NMR spectra were observed under cross-polarization, magic-angle spinning, and high-power dipolar decoupling (CP/MAS/DD) techniques. The 90° pulse was $4.5 \mu\text{s}$ for ^1H and ^{13}C (radio frequency strength for spin-locking was 56 kHz) while the spinning rate of MAS was around 6–7 kHz. A contact time of 1.0 ms was used for measuring CP/MAS spectra while the repetition time was 2 s. ^{13}C NMR spectra were also observed using a 90° single pulse excitation (SPE) method under MAS/DD conditions by using a repetition time of 2 s. ^{29}Si high-resolution solid-state NMR spectra were detected by a single 90° pulse sequence (pulse length of $4.5 \mu\text{s}$) with a repetition time of 30 s. under MAS/DD conditions. The chemical shift of the ^{13}C or ^{29}Si spectra was determined by taking the carbonyl carbon of solid glycine (176.03 ppm) or tetramethylsilane (0 ppm) as an external reference standard. ^1H MAS NMR spectra were observed by the Carr–Purcell–Meiboom–Gill (CPMG, $90^\circ_x - (t_1 - 180^\circ_y - t_1 - \text{echo})_n$) pulse sequence,³⁶ with a repetition time of 2 s and a 90° pulse length of $2.5 \mu\text{s}$. The $90^\circ - 180^\circ$ pulse spacing (t_1) in the CPMG sequence was 40 μs , n was varied, and 8 scans were used for each measurement. The same MAS rate was applied, and tetramethylsilane (0 ppm) was used as an external chemical shift reference.

3. Results and Discussion

3.1. Chemical Structures and Mobility of the WG–Alkoxy silane Network. The hydrolysis of alkoxy silanes catalyzed under acidic or basic conditions has been well documented.³² To minimize unwanted reactions prior to mixing with WG and therefore to promote extensive reaction with WG after the mixing, the alkoxy silanes were dissolved in the plasticizer phase (water and glycerol with a required amount) at neutral

Scheme 2. Various Chemical Species That Define the Extent of Condensation around a Silicon Center for SiA and SiB

pH conditions and then mixed with WG before compression molding. It is necessary to avoid reactions that will open the epoxy ring on the glycidoxy arm, as the epoxy group is important for reaction with amino and other functional groups in the WG system. In addition, significant condensation of the siloxane may prevent efficient reaction of the cross-linker with the WG for steric reasons. The ^{13}C solution NMR spectra and the assignment of pure SiA, SiB, and their hydrolyzed products after mixing with water (10 wt %) for 24 h or 7 days are shown in Figures 1 and 2. The chemical shift changed significantly after dissolving the siloxane in water, indicating interactions with water and some level of hydrolysis after 24 h. The persistence of peaks between 44–48 and 51–54 ppm indicates that the epoxy functional group was stable after hydration for 24 h. After hydration for 7 days, some minor resonances at 60–75 ppm in both SiA and SiB solutions did appear, suggesting hydrolysis of some minor amount of glycidoxy rings leading to new resonances reflecting the formation of $>CHOH$ and $-CH_2OH$ structures. For SiB, after hydration for 7 days, both the $Si-CH_3$ and the $Si-CH_2-$ resonances were split into several peaks, indicating that different Si structures were formed. When glycerol was involved in the SiA or SiB solution prior to mixing with WG, ^{13}C spectral characteristics were similar to those in water solution except for the presence of strong resonances at 73 and 64 ppm attributed to glycerol signals. The conclusion from this overall study was that only minimal ring opening of the epoxy group in SiA and SiB occurred when mixing with water/glycerol within 24 h.

The extent of hydrolysis and condensation for the silicon atoms was probed by ^{29}Si solution NMR spectroscopy. The chemical shift of silicon was determined by the number of siloxane bridges attached to a silicon atom. For alkoxysilanes the maximum condensation of a silicon center is determined by the number of hydrolyzable groups present on the silane. For the alkoxysilanes with two of three hydrolyzable alkoxy groups used in this work, they are often represented by the letters D and T, respectively.^{36–41} The number of siloxane bridges at a particular silicon center is then indicated by a number as shown in Scheme 2.

The ^{29}Si solution NMR spectra of SiA and SiB are shown in Figure 3. For pure SiA or SiB, the ^{29}Si resonances located at -41 or -6 ppm correspond to T^0 and D^0 , respectively, with no condensation. After hydration in water for 24 h, new resonances were observed at -50 ppm for SiA corresponding to the formation of T^1 . For SiB the resonance also splits into two after hydration, and the new resonance at -16 ppm was attributed to the formation of D^1 .^{37,41,42} Extending hydration for a longer period of time (ca. 7 days) caused further condensation as detected by ^{29}Si NMR spectroscopy. For SiA, only a minor amount of T^0 remained, and the T^1 species became predominant. The formation of T^2 was also observed, but there was no evidence of the T^3 structure being formed. All D^0 , D^1 , and D^2 structures^{37,41,42} coexisted in the SiB system after hydration for 7 days. However, there was no significant change in the viscosity of the solutions, and no precipitation was observed in either SiA or SiB solution even after hydration over 7 days. This

suggests that these hydrolyzed silane species did not form any high molecular weight products, which is also consistent with the narrow resonances in ^{13}C solution NMR spectra for both SiA and SiB solutions (Figures 1 and 2). These results indicate that during sample preparation time (within 24 h), although the SiA or SiB structures were hydrolyzed to some extent when mixing with the plasticizers (water and glycerol), there was no significant level of condensation and, most importantly, the epoxy groups were relatively stable prior to mixing with WG.

Thermal processing of the plasticized WG–SiA and WG–SiB systems resulted in the formation of thermoplastic sheets containing Si species in the WG matrix of the materials. The slightly acidic characteristics of the WG systems and the high temperatures (130 °C) during compression molding are expected to lead to further reaction of the silane. To identify whether SiA or SiB molecules were chemically incorporated into the WG matrix, the samples were subjected to sonication in water for 6 h. Only glycerol was extracted, the same as reported for cross-linked WG systems,⁹ but no SiA or SiB signals were detected in the water phase by solution NMR for most of the WG–SiA and WG–SiB materials except for WG–SiB-8% where a very small amount of SiB was indeed observed.

^{29}Si MAS NMR spectra of thermally processed WG–SiA and WG–SiB materials are shown in Figure 4. The wide distribution of the resonances suggested that different Si–O network structures were formed. The major ^{29}Si resonances were detected from -53 to -69 ppm for the WG–SiA-4% system, corresponding to the T^1 , T^2 , and T^3 structures in the network, while the minor peak at -43 ppm is due to the T^0 structure.^{36–41} The main peak at -16 ppm for WG–SiB-4% is attributed to D^1 with the minor peak at -24 ppm due to the D^2 structure.^{37,41,42} The low content of SiA or SiB in the materials contributed to the poor signal-to-noise ratio of these spectra. When the SiA content increased to 8%, the T^3 structure was the major component in the WG–SiA-8% system with some minor amount of T^2 , but the T^0 and T^1 structures disappeared. The results indicated that the increased concentration of SiA led to the predominant formation of T^3 structures due to a greater amount of SiA within the WG system, giving rise to extensive condensation. It requires three SiA segments to condense with a central SiA molecule to form T^3 structures, and this would become more likely when the content of SiA was increased. At a lower concentration of silane, WG–SiA-4%, less condensation was formed, implying that the silane species were well distributed within the WG matrix and did not form phase-separated structures. For the WG–SiB-8% system, the three peaks observed at -7 , -16 , and -25 ppm are due to D^0 , D^1 , and D^2 structures. The presence of D^0 indicates some SiB in the material has not been reacted or condensed, being consistent with excess SiB after material processing. In terms of siloxane condensation, the reactivity of the dialkoxy silane SiB should be lower than that of the trialkoxy silane, which may explain the presence of the free SiB in the WG–SiB-8% material. It appeared that at the higher SiB concentration, the lower reactivity of the SiB hindered the reaction between SiB bound to WG and the excess free SiB.

^{13}C CP/MAS NMR spectra of these thermally processed WG–SiA materials are shown in Figure 5A. The CP/MAS method is sensitive to the rigid components of the materials because the strong dipolar interactions in the rigid component would enhance the polarization transfer from protons to nearby carbons, thus enhancing the intensities of the carbon resonances. To obtain signals of the mobile component in the systems, the SPE spectra were detected with a repetition time as short as 2

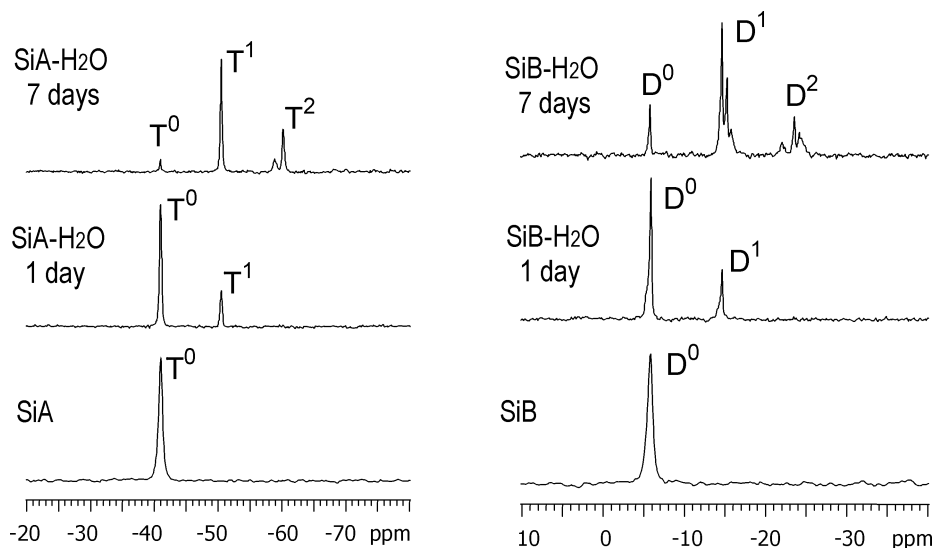


Figure 3. ^{29}Si solution NMR spectra of SiA or SiB and their products after hydration for 1 day or 7 days.

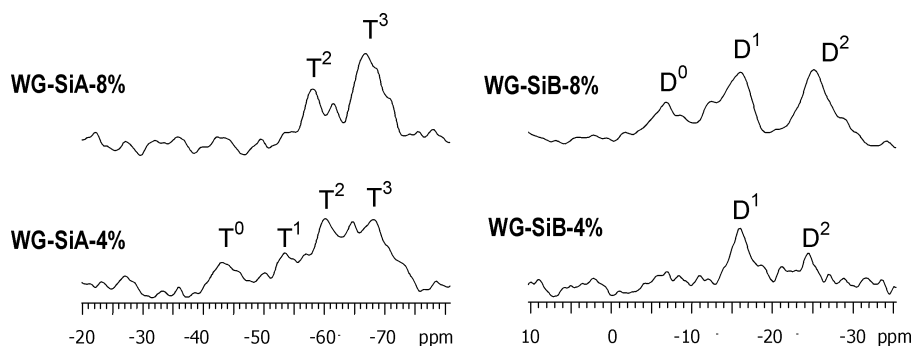


Figure 4. ^{29}Si high-resolution solid-state NMR spectra of WG-SiA or WG-SiB after thermal processing.

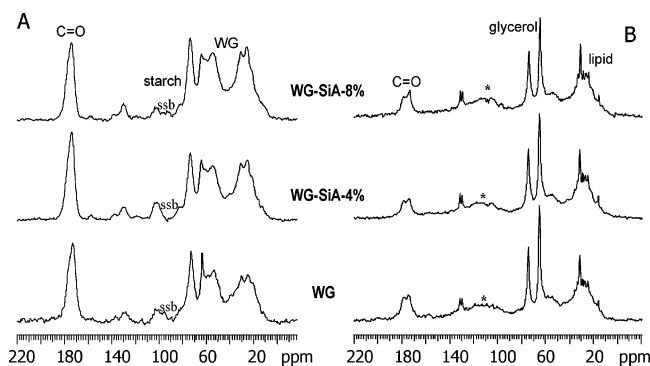


Figure 5. (A) ^{13}C CP/MAS and (B) SPE NMR spectra of WG-SiA materials.

s for the same systems and are shown in Figure 5B. The resonances of proteins (173, 54, 30, and 25 ppm) and residual starch (103 and 73–81 ppm, C-6 is overlapping with those of proteins) were observed in the CP/MAS spectra, and the assignment has been reported previously.^{6,7,43,44} Lipid and plasticized proteins were the major components detected in the SPE spectra. Glycerol signals at 73 and 64 ppm were detected in both CP/MAS and SPE spectra. These results were consistent with those reported previously. Note that no SiA signal was detected in the SPE spectra (Figure 5B). Although the T_0 structure was observed in Figure 4 for WG-SiA-4%, the amount could be too little to be observed, or the segments could associate with the WG matrix, thus becoming less mobile so that they were missed in the SPE spectra.

According to literature reports, the epoxy groups in both SiA and SiB would react with various amino groups in WG across

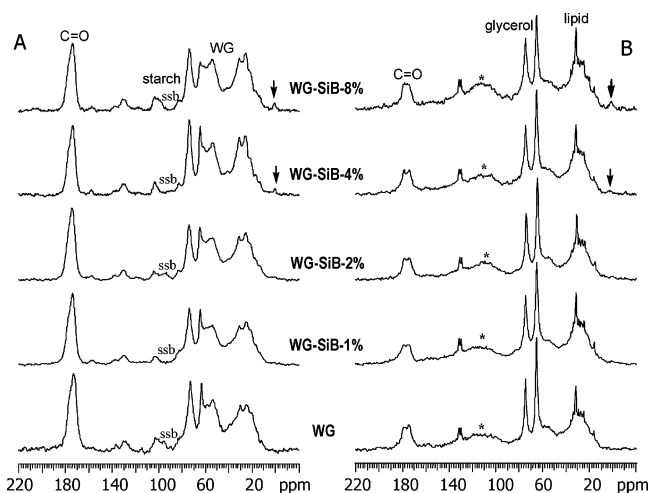


Figure 6. (A) ^{13}C CP/MAS and (B) SPE NMR spectra of WG-SiB materials.

a wide temperature range from room temperature upward.^{30,31,45,46} The hydroxyl groups of starch and glycerol could also react with the epoxy groups under similar conditions. However, all of the resonances derived from SiA in the ^{13}C CP/MAS spectra (Figure 5A) were heavily overlapped with those of WG and starch, making it impossible to detect the expected chemical changes brought about by nucleophilic ring opening of the epoxy group after thermal processing. For WG-SiB systems, the methyl ($\text{R}(\text{CH}_3)\text{Si}-$) resonance at around 0 ppm was observed, when the SiB content was 4%, in both CP/MAS (Figure 6A) and SPE spectra (Figure 6B), indicating that the SiB segments could remain in both the rigid and the mobile phases of the

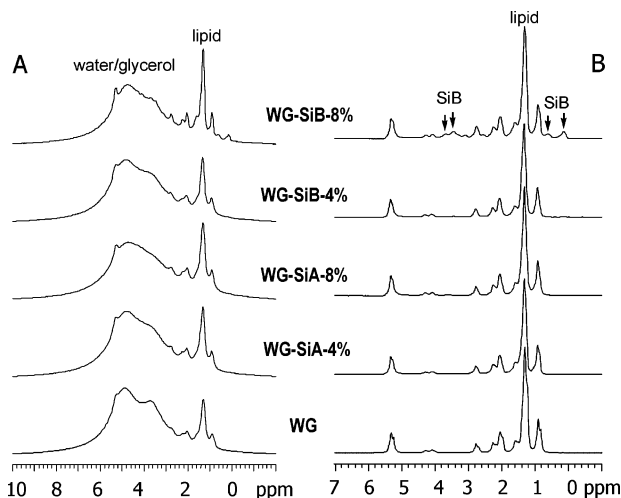


Figure 7. ^1H MAS NMR spectra of WG, WG-SiA-4%, WG-SiA-8%, WG-SiB-4%, and WG-SiB-8% samples detected by the CPMG pulse sequence with two typical τ times (A, 40 μs , and B, 10 ms) at which the n th echo appeared.

materials. The signals from SiB became more pronounced when the SiB content was increased to 8%, which is consistent with the mobile nature of SiB within the WG-SiB network and the presence of free SiB within the system.

The differences in mobility of the SiA and SiB components in the materials were also examined by ^1H MAS NMR experiments. Figure 7 shows the ^1H MAS NMR spectra of WG, WG-SiA, and WG-SiB systems measured by the CPMG pulse sequence using two typical τ times (A, 40 μs , and B, 10 ms) at which the n th echo appeared. Only very mobile components with long ^1H T_2 values could remain in the spectra with a long τ time while the rigid components with short ^1H T_2 values would be missed. The broad peaks in Figure 7A are assigned to plasticizers such as water and glycerol (3.7–4.5 ppm) while the sharp peaks at 0.9, 1.3, 2.0, 2.7, and 5.3 ppm are all attributed to the lipid phase.^{25,26} When a longer τ (10 ms) was used, the water and glycerol resonances disappeared, leaving mainly lipid signals as shown in Figure 7B, indicating that the lipid was more mobile than water and glycerol. This is consistent with the previously reported results.^{6,7} Note that ^1H signals attributed to SiB were only detected in WG-SiB-8% at both τ values (Figures 7A and 7B) and not for any other systems, including WG-SiB-4%. This indicates that the SiB signals observed here are only due to free or very mobile SiB molecules in WG-SiB-8% materials, most likely arising from the SiB that was not linked to WG or the WG-siloxane network. For all of the other systems it appeared that the SiA and SiB segments within WG were less mobile than the water and glycerol plasticizers after thermal processing.

The NMR results demonstrate that different network structures were indeed formed for WG-SiA and WG-SiB materials due to the different chemical nature of the two alkoxy silane compounds. A highly cross-linked network structure was formed for WG-SiA materials when the SiA content was higher, because of the restriction of molecular motion within the network. For WG-SiB systems, linear linkages were produced within the SiB component of the network, and the SiB segments were relatively mobile although they were not as mobile as the plasticizers. These structure variations should be linked intimately to the material performance.

3.2. Molecular Motions and T_g Transitions of WG-Alkoxy silane Materials. The motional dynamics of WG-alkoxy silane networks were studied using DMA techniques, and

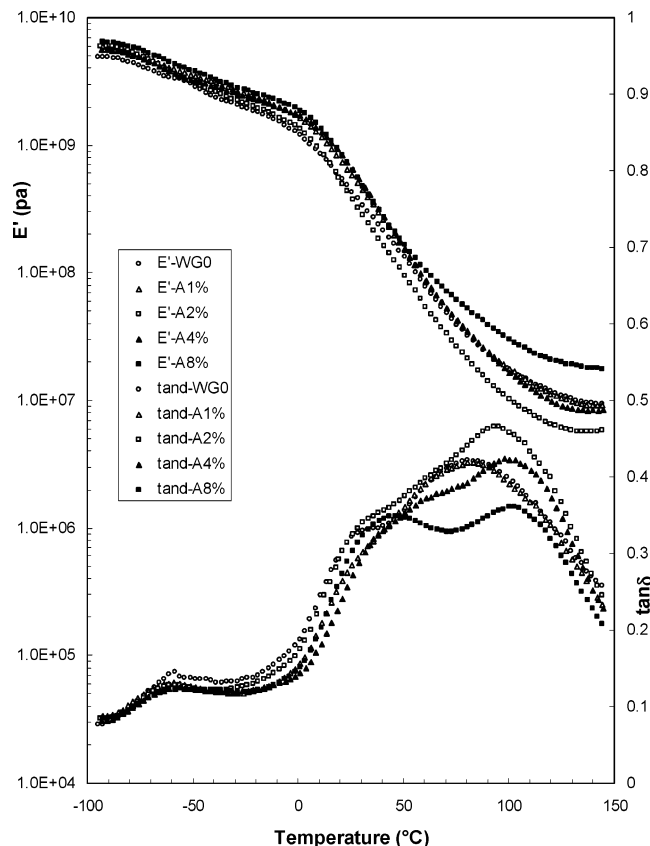


Figure 8. Storage modulus (E') and $\tan \delta$ of WG-SiA materials: WG-0 (\circ), WG-SiA-1% (Δ), WG-SiA-2% (\square), WG-SiA-4% (\blacktriangle), and WG-SiA-8% (\blacksquare).

the results for WG-SiA and WG-SiB systems are shown in Figures 8 and 9, respectively. The DMAs of the WG-SiA and WG-SiB materials were similar to those of plasticized WG; as the temperature increased, the E' (storage modulus) decreased slowly and then dropped quickly at a typical temperature due to the glass transition of the systems. The onset of this E' decrease was taken as the start of T_g transitions, while strong $\tan \delta$ peaks were observed corresponding to the T_g transitions. At around -60°C , a minor $\tan \delta$ peak was also obtained in conjunction with an E' onset due to β transitions of the WG materials.^{4–10}

When adding either SiA or SiB to the WG systems, E' in the low-temperature range (below T_g) was enhanced in general as compared to those of WG. However, such systems displayed an interesting behavior at higher temperatures far above T_g . The E' data were lower than those of WG when applying 1% and 2% alkoxy silanes to the systems, recovered when 4% of alkoxy silanes was used, and then exhibited a significant E' improvement with 8% of alkoxy silanes in the systems. The E' onset corresponding to T_g transitions also shifted to higher temperatures when alkoxy silanes were introduced into the WG materials. The difference in using either SiA or SiB was minimal. Although a certain amount of water ($\sim 12\%$) was present in the systems, a transition due to ice melting was not observed at around 0°C , indicating that the water molecules were strongly hydrogen-bonded with protein macromolecules and did not exist as free water as described in previous reports.⁷

The curves of $\tan \delta$ versus temperature in both Figures 8 and 9 displayed a significant three-peak character especially when the content of either SiA or SiB was high in the materials. The minor peak at around -60°C was consistent with the β -transitions, while the two major $\tan \delta$ peaks at high temper-

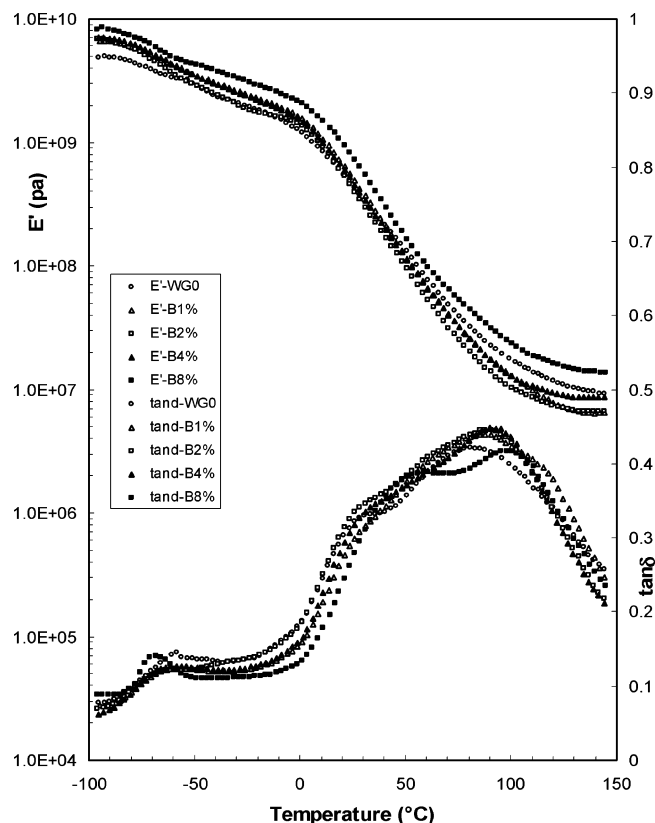


Figure 9. Storage modulus (E') and $\tan \delta$ of WG–SiB materials: WG-0 (○), WG–SiB-1% (△), WG–SiB-2% (□), WG–SiB-4% (▲), and WG–SiB-8% (■).

Table 1. DMA Results of WG–SiA and WG–SiB Systems^a

samples	$\tan \delta_1$ (°C)	$\tan \delta_1$ max	$\tan \delta_2$ (°C)	$\tan \delta_2$ max	$\tan \delta_3$ (°C)	$\tan \delta_3$ max
WG	–58	0.145	26	0.305	82	0.419
WG–SiA-1%	–59	0.131	29	0.274	82	0.418
WG–SiA-2%	–59	0.128	34	0.344	94	0.464
WG–SiA-4%	–59	0.124	41	0.321	99	0.421
WG–SiA-8%	–59	0.123	46	0.346	100	0.358
WG–SiB-1%	–61	0.122	32	0.315	90	0.435
WG–SiB-2%	–60	0.123	33	0.330	91	0.441
WG–SiB-4%	–60	0.126	34	0.321	91	0.450
WG–SiB-8%	–68	0.141	45	0.335	102	0.405

^a Temperature error ~ 1 –2 °C.

atures are likely to be the T_g transitions of the WG–alkoxysilane networks. The temperatures where the $\tan \delta$ peaks appeared and the $\tan \delta$ maximum values are listed in Table 1. The SiA displayed a minimal effect on the temperatures where the β transitions occurred; however, the maximum of the $\tan \delta$ peaks decreased as the content of SiA increased (0.145 for WG, but 0.128 for WG–SiA-2% and 0.123 for WG–SiA-8%), suggesting some level of motional restriction to the β transitions. A more significant influence on the β transitions occurred when applying 8% of SiB to the WG materials, where the $\tan \delta$ peak shifted to -68 °C while the $\tan \delta$ maximum reverted to the level of WG, suggesting an increase in motion within the system due to the presence of very mobile SiB molecules.

As reported previously,^{6–8} plasticized WG materials usually display a wide distribution of molecular mobility. Generally multiphase structures with varied mobility were observed. The less plasticized proteins and residual starch were defined as the rigid phase, plasticized proteins and starch and some of the plasticizers were defined as the intermediate phase, and the

mobile phase consisted of lipid and plasticizers. The two major $\tan \delta$ peaks of the WG at temperatures of 82 and 26 °C could be attributed to the T_g transitions of the less plasticized (rigid) and plasticized phases of the materials, respectively. Increasing the amount of alkoxysilanes in the systems resulted in both transitions shifting to higher temperatures. Meanwhile, the maximum values of the $\tan \delta$ peaks were also modified; the values increased slightly when the content of alkoxysilanes increased but then decreased when further increasing the content of alkoxysilanes. The results indicate that a low content of alkoxysilanes promoted increased molecular motions while a further increase in the content of alkoxysilanes caused a significant motional restriction for the macromolecules in both phases. These changes in molecular motion strongly suggest that a cross-linked network was indeed formed when either SiA or SiB content was increased.

A further point to note is that the $\tan \delta$ maximum values corresponding to these T_g transitions in WG–SiA were lower than those of the WG–SiB materials. The different T_g transitions of WG–SiA and WG–SiB were attributed to the different network structures formed by the silanes depending on their chemical reactivity. In short, the highly cross-linked network structures were formed in WG–SiA materials when the SiA content was sufficiently high, leading to more motional restriction at the T_g transitions. However, SiB with a dialkoxysilyl structure should produce linear condensed segments in the WG–SiB network, and the materials would be more mobile than WG–SiA, especially at temperatures above their T_g .

3.3. Mechanical Performance of WG–Alkoxysilane Materials. The formation of WG–alkoxysilane networks also significantly modified the mechanical properties of the plasticized WG materials. The results of tensile strength and elongation at breakage of the WG–SiA and WG–SiB systems are shown in Figures 10 and 11. With 1% of either SiA or SiB in the systems, the tensile strength of the materials was weakened as compared to that of WG at RH = 50%. When the amount of the alkoxysilanes further increased, the tensile strength at RH = 50% increased significantly (up to 60%) for WG–SiA systems, but only around 10% strength improvement was obtained for the WG–SiB system. The elongation at breakage for the materials increased from 55% (for WG) to 150–160% when 1% of the alkoxysilane was introduced into WG. Increasing the amount of alkoxysilanes resulted in some decrease in elongation at RH = 50%, but the values still remained at a level of 50–60% (similar to that of WG) even when 8% of the alkoxysilanes were used.

At the higher humidity exposure conditions (RH = 85%) all materials contained a similar level of moisture ($\sim 22\%$), but their mechanical properties were quite different. The tensile strength of both WG–SiA and WG–SiB systems were enhanced markedly (by up to 65–80%) when the content of the alkoxysilanes increased at RH = 85%, conversely the elongation at breakage decreased with higher loadings of alkoxysilanes. Generally for WG systems at the higher humidity, more moisture is absorbed by the material, resulting in additional plasticizing to the WG and thus lower tensile strength and higher elongation values for the materials. But the presence of alkoxysilanes enhanced the tensile strength and reduced the elongation of the systems even when moisture content remained at a similar level. The results suggest the enhancement of hydrostability of the networks; the same amount of plasticizers produced a much lower level of plasticizing when WG–siloxane network structures were formed.

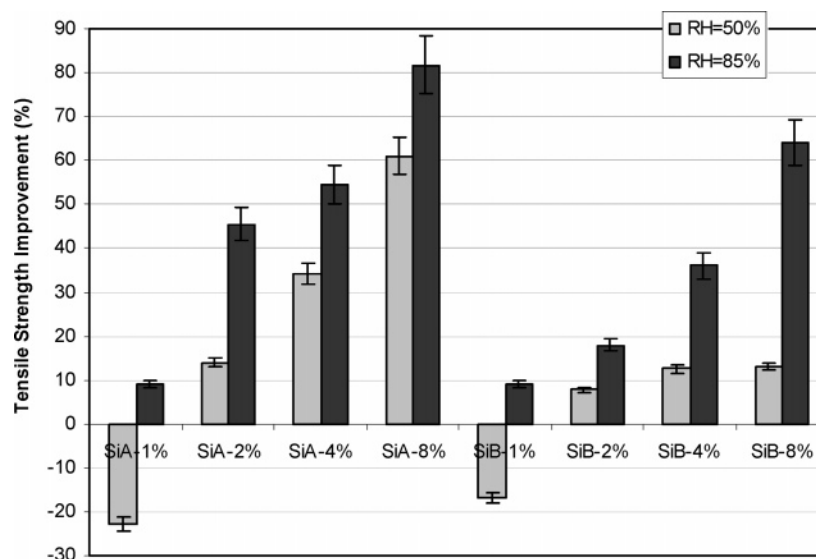


Figure 10. Improvement in tensile strength of WG-SiA and WG-SiB as compared to pure WG after conditioning at RH = 50% and 85%.

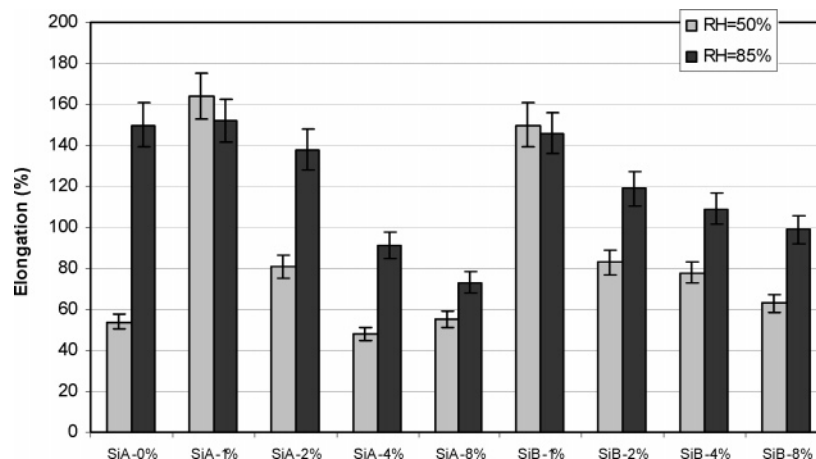


Figure 11. Elongation at breakage data for WG-SiA and WG-SiB after conditioning at RH = 50% and 85%.

The mechanical performance of WG-SiA and WG-SiB can be explained by different network structures formed in the two systems. As already discussed in this report, there was a wide distribution of silicon structures in the systems that was characterized in ^{29}Si CP/MAS NMR spectra (Figure 4; WG-SiA, T^0 , T^1 , T^2 , and T^3 ; WG-SiB, D^0 , D^1 , and D^2). When the amount of the alkoxyxilanes was low (ca. 1%), it was less likely that significant quantities of alkoxyxilane segments could meet to undergo the condensation reaction that leads to the formation of the siloxane network during thermal processing. From these results it appeared that the alkoxyxilanes at low concentration were grafted onto the protein molecules and act as an additional plasticizer to the systems, thus generating a weaker tensile strength and a high elongation for the materials at RH = 50%. When the amount of the alkoxyxilanes increased, there was an increased tendency for the SiA or SiB segments to condense with each other to form linkages through the whole polymer matrix. This resulted in an enhancement of tensile strength and a decrease in material elongation. However it should be remembered that the alkoxyxilane networks were at least as flexible as the plasticized WG at RH = 50%, so it can be concluded that higher tensile strengths in WG systems can be achieved with the addition of alkoxyxilanes without sacrificing elongation at breakage (Figures 10 and 11). At higher humidity (RH = 85%) the plasticizing effect from the additional moisture content dominates the properties of the WG systems, but the

higher content of the silane cross-linker reduces this effect to give a more hydrostable material. This is clearly demonstrated by higher tensile strengths and lower elongation values with increasing silane concentration.

4. Conclusions

Polymer grafting alkoxyxilanes onto plasticized wheat gluten macromolecules via condensation reactions occurred under mild conditions, and further thermal processing resulted in the formation of WG-alkoxyxilane networks. The materials contained a wide distribution of Si structures, which were based on the different contents and different chemical structures of the alkoxyxilanes used in the systems. When the content of alkoxyxilanes was low in the systems, the alkoxyxilane molecules were mainly grafted onto WG molecules with less opportunity to form linkages between these alkoxyxilane segments. This type of modification of the WG system provided an additional plasticizing effect at RH = 50% but at a higher RH of 85% the larger content of water dwarfed the plasticizing effect from the alkoxyxilane components.

The formation of linkages between the alkoxyxilanes segments and the WG-alkoxyxilanes network occurred when the amount of alkoxyxilanes reached a sufficient level in the systems. A significant motional restriction was produced for these materials,

and their T_g was also shifted to higher temperatures. A remarkable improvement in tensile strength was obtained for the cross-linked networks in conjunction with a reduction in elongation when the alkoxysilane content was increased. However, at RH = 50% the elongation values still remained at a level higher than that of plasticized WG itself because the network was relatively flexible. The strength improvement in the WG–SiA system was more pronounced at both RH = 50% and RH = 85%, corresponding to the formation of highly cross-linked stable structures. For WG–SiB systems, the mobility of the SiB segments caused a lower strength improvement but longer elongation values for the materials compared to SiA due to the linear linkages formed in the WG–SiB network.

This work provides a clear demonstration that the mechanical performance of WG materials can be modified through the formation of different chemical and network structures with alkoxysilanes and a variation in molecular motions of the WG macromolecules. A particularly promising aspect for future work resulting from this study will be utilizing the modification of the WG system without extensive cross-linking when using a low concentration of silane. Such modification opens up the use of different organosilanes or other appropriate organometallic reagents that can link to the modified wheat gluten or other plant proteins with the aim of controlling properties such as tensile strength, hydrostability, or hydrophobicity and toughness.

References and Notes

- Ching, C.; Kaplan, D.; Thomas, E. *Biodegradable Polymers and Packaging*; Technomic Publishing: Basel, Switzerland, 1993.
- Wool, R. P.; Sun, X. S. *Bio-based Polymers and Composites*; Elsevier Academic Press: Amsterdam, 2005.
- Biodegradable Polymers for Industrial Applications*; Smith, R., Ed.; CRC Press: Boca Raton, FL, 2005.
- Zhang, X.; Bugar, I.; Lourbakos, E.; Beh, H. *Polymer* **2004**, *45*, 3305–3312.
- Zhang, X.; Do, M.; Lourbakos, E. *Polym. Prepr.* **2005**, *46*, 321–322.
- Zhang, X.; Bugar, I.; Do, M.; Lourbakos, E. *Biomacromolecules* **2005**, *6*, 1661–1671.
- Zhang, X.; Do, M.; Hoobin, P.; Bugar, I. *Polymer* **2006**, *47*, 5888–5896.
- Zhang, X.; Hoobin, P.; Bugar, I.; Do, M. *Biomacromolecules* **2006**, *7*, 3466–3473.
- Zhang, X.; Hoobin, P.; Bugar, I.; Do, M. *J. Agric. Food Chem.* **2006**, *54*, 9859–9865.
- Zhang, X.; Do, M.; Dean, K.; Hoobin, P.; Bugar, I. *Biomacromolecules* **2007**, *8*, 345–353.
- Means, G. E.; Feeney, R. E. *Chemical Modification of Proteins*; Holden-Day: San Francisco, CA, 1971.
- Wong, S. S. *Chemistry of Protein Conjugation and Cross-Linking*; CRC Press, Boca Raton, FL, 1993.
- Scheyer, L. E.; Polsani, M. *Starch/Staerke* **2000**, *5*, 420–422.
- Lutolf, M. P.; Hubbell, J. A. *Biomacromolecules* **2003**, *4*, 713–722.
- Woerdeman, D. L.; Veraverbeke, W. S.; Parnas, R. S.; Johnson, D.; Delcour, J. A.; Verpoest, I.; Plummer, C. J. G. *Biomacromolecules* **2004**, *5*, 1262–1269.
- Micard, V.; Belamri, R.; Morel, M.-H.; Guilbert, S. G. *J. Agric. Food Chem.* **2000**, *48*, 2948–2953.
- Hernandez-Munoz, P.; Villalobos, R.; Chiralt, A. *Food Hydrocolloids* **2004**, *18*, 403–411.
- Ghorpade, V. M.; Li, H.; Gennadios, A.; Hanna, M. A. *Trans. ASAE* **1995**, *38*, 1805–1808.
- Park, S. K.; Bae, D. H.; Rhee, K. C. *J. Am. Oil Chem. Soc.* **2000**, *77*, 879–883.
- Rhim, J. W.; Gennadios, A.; Handa, A.; Weller, C. L.; Hanna, M. A. *J. Agric. Food Chem.* **2000**, *48*, 4937–4941.
- Lieberman, E. R.; Guilbert, S. G. *J. Polym. Sci., Polym. Symp.* **1973**, *41*, 33–43.
- Parris, N.; Coffin, D. R. *J. Agric. Food Chem.* **1997**, *45*, 1596–1599.
- Galiotti, G.; di Gioia, L.; Guilbert, S.; Cuq, B. *J. Dairy Sci.* **1998**, *81*, 3123–3130.
- Marquie, C.; Aymard, C.; Cuq, J. L.; Guilbert, S. *J. Agric. Food Chem.* **1995**, *43*, 2762–2767.
- Marquie, C. *J. Agric. Food Chem.* **2001**, *49*, 4676–4681.
- Happich, W. F.; Windus, W.; Naghski, J. *Text. Res. J.* **1965**, *35*, 850–852.
- Di Monica, G.; Marzona, M. *Text. Res. J.* **1971**, *41*, 701–705.
- Tropini, V.; Lens, J.-P.; Mulder, W. J.; Silvestre, F. *Ind. Crops Prod.* **2003**, *20*, 281–289.
- Kuijpers, A. J.; Engbers, G. H. M.; Feijen, J.; de Smedt, S. C.; Meyvis, T. K. L.; Demeester, J.; Krijgsveld, J.; Zaat, S. A. J.; Dankert, J. *Macromolecules* **1999**, *32*, 3325–3333.
- Van Wachem, P. B.; Zeeman, R.; Dijkstra, P. J.; Feijen, J.; Hendriks, M.; Cahalan, P. T.; van Luyn, M. J. A. *J. Biomed. Mater. Res.* **1999**, *47*, 270–277.
- Sung, H.-W.; Huang, D.-M.; Chang, W.-H.; Huang, R.-N.; Hsu, J.-C. *J. Biomed. Mater. Res.* **1999**, *46*, 520–530.
- Plueddemann, E. P. *Silane Coupling Agents*; Plenum Press: New York, 1982.
- Furukawa, H.; Kato, Y.; Ando, M.; Inoue, M.; Lee, Y. K.; Hazan, I.; Omura, H. *Prog. Org. Coat.* **1994**, *24*, 81–89.
- Narkis, M.; Tzur, A.; Vaxman, A. *Polym. Eng. Sci.* **1985**, *25*, 857.
- Dow Corning Silane. <http://www.dowcorning.com/content/silanes> (accessed May 13, 2007).
- Williams, E. A. *Recent Advances in Silicon-29 NMR Spectroscopy*; Annual Reports on NMR Spectroscopy 15; Academic Press: London, 1983.
- Joseph, R.; Zhang, S.; Ford, W. T. *Macromolecules* **1996**, *29*, 1305–1312.
- Alam, T. M.; Assink, R. A.; Loy, D. A. *Chem. Mater.* **1996**, *8*, 2366–2374.
- Lindner, E.; Jager, A.; Schneller, T.; Mayer, H. A. *Chem. Mater.* **1997**, *9*, 81–90.
- Salon, M.-C. B.; Abdelmouleh, M.; Boufi, S.; Belgacem, M. N.; Gandini, A. *J. Colloid Interface Sci.* **2005**, *289*, 249–261.
- Young, S. K.; Jarrett, W. L.; Mauritz, K. A. *Polymer* **2002**, *43*, 2311–2320.
- Balonneau, F.; Thorne, K.; Mackenzie, J. D. *Chem. Mater.* **1989**, *1*, 554–558.
- Belton, P. S.; Duce, S.; Colquhoun, I. J.; Tatham, A. S. *Magn. Reson. Chem.* **1988**, *26*, 245–251.
- Calucci, L.; Forte, C.; Galleschi, L.; Geppi, M.; Ghiringhelli, S. *Int. J. Biol. Macromol.* **2003**, *32*, 179–189.
- Sung, H.-W.; Hsu, C.-S.; Lee, Y.-S.; Lin, D.-S. *J. Biomed. Mater. Res.* **1996**, *31*, 511–518.
- Sung, H.-W.; Huang, R.-N.; Huang, L.; Tsai, C.-C.; Chiu, C.-T. *J. Biomed. Mater. Res.* **1998**, *42*, 560–567.

BM070290C